Clays and Clay Minerals, Vol. 44, No. 5, 624–634, 1996.

CATION EXCHANGE CAPACITY OF LAYER SILICATES AND PALAGONITIZED GLASS IN MAFIC VOLCANIC ROCKS: A COMPARATIVE STUDY OF BULK EXTRACTION AND *IN SITU* TECHNIQUES

P. SCHIFFMAN[1] AND R. J. SOUTHARD[2]

[1] Dept of Geology, University of California, Davis, Davis, CA 95616
[2] Dept of Land, Air and Water Resources, University of California, Davis, Davis, CA 95616

Abstract—The cation exchange capacities (CEC) and extractable cations in smectite, corrensite and palagonitized glass from hydrothermally-altered pillow lavas and hyaloclastite breccias were measured by both bulk wet chemical and *in situ* microanalytical techniques. Smectite has CEC's between 60 and 120 meq/100 g, palagonitized glass between 30 and 60 meq/100 g, and corrensite approximately 35 meq/100 g as determined by the *in situ* CsCl-exchange method. These experiments generally verify that Cs exchanges for those cations that are presumed (from the stoichiometry implied by microprobe analyses) to occupy interlayer sites in sheet silicates. Results of conventional CEC determinations are consistent with those determined by the *in situ* experiments: the individual microanalytical values for smectite and palagonitized glass bracket the bulk CEC values. The *in situ* experiments imply that Mg is the major extractable cation in smectite, Ca in corrensite, and both Mg and Ca in the palagonitized glass. We speculate that discrepancies between the equivalents of extractable cations predicted from elemental analysis and the equivalents of Cs sorbed may be due to the presence of charge-balancing protons that are not detected by the microprobe analyses. The sum of equivalents of cations extracted by NH_4-acetate is about the same as the CEC determined by both the *in situ* and the bulk methods. Cation proportions indicated by NH_4-acetate extractions from bulk samples are also generally consistent with the *in situ* results for all elements except Mg, which is a minor leachate of the NH_4-acetate extractions in all the samples. To explain this discrepancy, we propose that 1) Mg may occupy structural sites within palagonitized glass, which inhibit its extraction by NH_4 or Cs, and/or 2) there is a significant quantity of smectite, unsampled by the electron microprobe analyses, which contains insignificant interlayer Mg.

Key Words—Cation Exchange Capacity, Corrensite, Electron microprobe analysis, Extractable cations, Palagonite, Smectite.

INTRODUCTION

Incipient alteration of mafic volcanic rocks, particularly in hydrothermal environments, entails the palagonitization of glass with concomitant crystallization of layer silicates (primarily smectite) and zeolites. Palagonitization is also an important process in the weathering/saprolitization of mafic volcanic rocks. Geologists traditionally characterize the *in situ* properties of palagonitic materials such as their textures and mineralogies with light, scanning or transmission electron microscopes (Hay and Iijima 1968; Dimroth and Lichtblau 1979; Jakobsson and Moore1986; Thorseth et al. 1991; Zhou et al. 1992) and their compositional variations with electron microprobes (e.g, Staudigel and Hart 1983; Furnes 1984; Zhou and Fyfe 1989; Jercinovic et al. 1990; Thorseth et al. 1995). Soil scientists typically measure bulk properties such as size fraction distribution, the structural response to chemical and thermal treatments as determined by X-ray diffraction (XRD) and chemical characteristics such as cation exchange capacity (CEC) and extractable cations (Singer 1974; Golden et al. 1993; Berkgaut et al. 1994). Collectively, these data have documented that profound compositional, mineralogical and textural heterogeneities typically accompany the palagonitization of mafic glasses. The process of palagonitization is thought to affect: 1) the composition of seawater and the oceanic crust (Staudigel and Hart 1983); 2) the spectral properties of planetary surfaces (Golden et al. 1993); 3) the sorption/retention properties of glass-hosted, nuclear-waste repositories (Jercinovic et al. 1990); and 4) the biogeochemical cycling of nutrients in soils developed on volcanic protoliths.

We examined some compositional effects accompanying the palagonitization of mafic volcanoclastic rocks, also known as metabasites, from an exhumed stratigraphic section of a Pliocene aged submarine seamount exposed on La Palma, in the Canary Islands. Published microprobe data on the composition of trioctahedral smectite formed during hydrothermal alteration of these rocks (Schiffman and Staudigel 1995) support the hypothesis that interlayer sites are dominantly filled with Mg. The present study was initiated to test this hypothesis by measuring the cation exchange capacity (CEC) and extractable cations of this smectite with both traditional bulk methods and an *in situ* method using the electron microprobe (Hillier and Clayton 1992). Since the bulk clay fractions of hyaloclastitic samples contain appreciable palagonitized

glass, we also measured its *in situ* properties. Previous studies (Singer 1974; Berkgaut et al. 1994) have shown that "palagonite" has a relatively high CEC (60 to 100 meq/100 g, as measured on bulk clay fractions), although the relative contribution of exchangeable cations from dominantly amorphous material versus crystalline layer silicates has not been previously explored.

In this paper, the term palagonite is used in reference to a bulk sample of metabasite which contains a mixture of palagonitized glass, authigenic minerals: smectite, corrensite, zeolites, carbonates and Fe-Ti oxides and phosphates, and primary minerals: plagioclase feldspars, clinopyroxene and olivine.

GEOLOGICAL SETTING

The Pliocene Seamount Series is a submarine basement complex on La Palma, in the Canary Islands (Staudigel 1981; Staudigel and Schmincke 1984). Samples for this study were collected from surface outcrops along the Barranco de las Angustias, where an approximately 3.5 km thick stratigraphic section, predominantly composed of alkaline, mafic pillow lavas and volcanoclastites, is exposed. The exact locations of the 5 samples examined in this study are shown in Schiffman and Staudigel's Figure 1 (1995).

Submarine hydrothermal metamorphism of the Seamount Series has resulted in a relatively complete low P-T facies series, with implied thermal gradients of 200 to 300 °C/km, serially encompassing the zeolite, prehnite-pumpellyite and greenschist facies (Schiffman and Staudigel 1994). Alteration within the upper 800 m of the Seamount Series extrusive section, where all but one of the samples examined for this study were collected, is characterized by the presence of palagonite containing, palagonitized glass, smectite, apatite, calcite and zeolites, including analcime and thompsonite-natrolite solid solution. Zeolites and calcite mostly fill veins and vesicles, as well as cement pore space in palagonitized hyaloclastites. Smectite occurs primarily as vesicle linings and as a recrystallization product of palagonite. In the samples examined for this study, clinopyroxenes are fresh, olivines are ubiquitously replaced by smectite and volcanic glass is completely palagonitized. Plagioclase may be fresh or partially zeolitized. Corrensite replaces smectite as the dominant layer silicate mineral at depths from approximately 800 to 1100 m in the extrusive section (Schiffman and Staudigel 1994).

ANALYTICAL METHODS

Preparation of clay and silt size fractions for XRD analysis utilized standard procedures (Whittig and Allardice 1986). Rock fragments ground in a micronizing mill were treated with a buffered (pH 5.0) sodium acetate solution to remove carbonate. The < 2 μm and 2 to 10 μm size fraction were separated by centrifugation in dilute sodium carbonate solution, and the fractionated clays were plated onto porous ceramic tiles maintained under vacuum suction (Kinter and Diamond 1966). Duplicate tiles, saturated with 0.5 *M* $MgCl_2$, were prepared for each sample. One clay mount was washed with distilled water, air-dried overnight and then analyzed. It was then saturated with 1 *M* KCl, dried overnight and analyzed. Finally it was heated at 550 °C for 1 h prior to analysis. The other mount was solvated with glycerol, dried overnight, and then analyzed. The mounts were analyzed on a Diano 8000 X-ray diffractometer operated at 50 kV and 15 mA, producing CuKα radiation, with a graphite monochromator. The samples were routinely scanned between 2 and 30 °2θ) at 2 °2θ/min.

Backscattered electron (BSE) imaging and mineral compositional analyses were performed on doubly polished, carbon-coated, thin sections using a Cameca SX-50 electron microprobe. Quantitative, wavelength dispersive, analyses of smectite, corrensite and palagonitized glass were performed at 15 keV and 5 to 10 nA beam current using a rastered, defocused beam with an approximately 10 μm diameter. The following silicate, oxide and chloride standards were used in conjunction with conventional ZAF matrix corrections: omphacite (Na), tremolite (Mg), anorthite (Al), tremolite (Si), orthoclase (K), wollastonite (Ca), TiO_2 (Ti), rhodonite (Mn), fayalite (Fe) and CsCl (Cs). The Cs-Lα line was measured using a PET dispersive crystal. Each analyte line and its corresponding background were measured for 10 s. A chlorite working standard (Bilgrami and Howie 1960) was routinely analyzed at the beginning of each session to ensure accuracy.

The *in situ* CEC's of layer silicates and palagonite were determined using the "Cs-staining" method outlined by Hillier and Clayton (1992). After removing the carbon coating, a solution of 1 *M* CsCl was applied by eyedropper to the surface of polished thin sections. After 3 h, thin sections were thoroughly rinsed and then soaked in distilled water for an additional 4 h. The latter was necessary to ensure that there were no residual precipitates of CsCl, which are easily detected by BSE examination. After air-drying, thin sections were carbon-coated again and re-analyzed, using CsCl as a calibration standard. As explained in Hillier and Clayton (1992), for each analysis:

$$\textit{in situ}\ \text{CEC (meq/100 g)} = (1000 \times \text{wt\% } Cs_2O)/(282/2) \quad [1]$$

Although Hillier and Clayton (1992) suggested that the CsCl solution should be applied overnight prior to rinsing, we found that 3 h was adequate for the La Palma samples. Cs-exchange was as complete for layer silicates and palagonitized glass on newly polished surfaces created after the outer 10 to 15 microns of a previously CsCl-saturated sample was removed.

Table 1. Lithology, mineralogy, and cation exchange characteristics of La Palma metabasites.

Sample	Lithology	Mineralogy†	Cation exchange capacity (meq/100 g)				
			In situ layer silicate mineral‡	*In situ* palagonitized glass‡	Excess salt method§	Sum of bulk extractable cations¶	% carbonate††
Lp743f	Interpillow hyaloclastite matrix	sm + pa (1:3)	120 (12)	61 (12)	77	48	0.15
Lp747a	Pillow basalt interior	sm	60 (6)	none	50	56	1.10
Lp754k	Interpillow hyaloclastite matrix	sm + pa (1:1)	69 (7)	33 (14)	55	95	0.38
Lp758b	Pillow basalt interior	co	35 (10)	none	52	35#	12.81
Lp762h	Hyaloclastite pillow breccia	sm + pa (3:1)	85 (6)	44 (14)	79	62	0.67

† Mineralogy determined by combination of XRD of <2 micron and 2 to 10 micron fractions and microprobe analysis. Key: sm = smectite; pa = palagonitized glass; co = corrensite; ( ) = ratio of smectite to palagonitized glass estimated by petrography.

‡ CEC determined by microprobe analyses of CsCl-saturated material. Mean value of the number of spot analyses given within parentheses.

§ CEC determined by excess salt method on <2 micron size fraction.

¶ Sum of Ca, K, Na and Mg cations extracted with 1 M NH4 acetate at pH 7.0 on <2 mm fraction, adjusted for dissolution of $CaCO_3$.

The high carbonate content in this sample precludes the adjustment for extractable Ca due to dissolution of $CaCO_3$.

†† CO_2 measured manometrically after reaction with 2 M HCL for 30 min.

Conventional CEC was determined using the "excess salt" method (Jackson 1979). Clay size fractions (< 2 μm) were saturated with 1 *M* $CaCl_2$ and then equilibrated with 0.01 *M* $CaCl_2$. The Ca was replaced by 1 *M* $MgCl_2$, and measured by atomic absorption. The CEC value presented in Table 1 is the mean of 2 or 3 replications that have a spread of generally less than 10%.

Extractable cations were measured on ground, bulk material (of the < 2 mm size fraction) leached with 1 *M* NH_4-acetate at pH 7.0. The Ca^{2+} and Mg^{2+} were measured by atomic absorption; K^+ and Na^+ were measured by flame photometry. The $CaCO_3$ content of the < 2 mm size fraction was measured by manometric determination of evolved CO_2 (Soil Survey Staff 1992) after reaction with 2 *M* HCl for 30 min.

RESULTS

XRD

In a paragenetic study of the hydrothermal layer silicates from the La Palma Seamount Series, Schiffman and Staudigel (1995) reported XRD data on the clay size fractions of the 5 samples used in the present study. Results on these 5 samples are summarized in Table 1. All contain a single layer silicate mineral. Four of the 5 samples contain trioctahedral smectite and the fifth (LP 758B, from deeper in the stratigraphic section) contains corrensite. Although 3 of the 5 samples, LP 743f, 754k and 762 h, are hyaloclastites and contain significant quantities of palagonitized glass, the samples also all contain abundant, well-crystallized smectite. Strong diffraction peaks from the smectite preclude the positive identification of palagonitized glass by XRD studies (Singer 1974; Zhou et al. 1992). The XRD patterns of the silt size (2 to 10 μm) fractions indicate that the silts contain layer silicates identical to those from the clay fraction.

BSE Petrography/X-ray Dot Mapping

The BSE micrographs and X-ray dot maps depicting the textural and compositional relationships of palagonitized glass and layer silicates are presented in Figures 1 through 4. Petrographic studies of palagonitized glasses have traditionally employed plane polarized light techniques, which image absorption colors that reflect corresponding compositional variations. The BSE technique, which has not been widely applied to the study of palagonite, produces images of gray-level variations, which reflect compositional variations, but can also be readily correlated with X-ray dot maps of the same area (Figures 2–4).

In the 3 hyaloclastites (LP743f, LP754k and LP762h), palagonitized glass accounts for over 50% of the sample volume. Figure 1 depicts some typical textural relationships in these hyaloclastites. Clasts are composed of palagonitized glass that is often concentrically zoned, either around amygdules filled by smectite and zeolites (Figure 1a, upper right) or the margins of the fragments themselves (Figure 1b). Locally, it is difficult to ascertain whether smectite aggregates are amygdaloidal, or if they recrystallized from palagonitized glass (Figure 1a, lower left).

Micrographs of CsLα X-ray dot maps collected from the CsCl-treated polished thin sections provide powerful qualitative information on the relative CEC of the various mineral components of the hyaloclastites. Figure 2 depicts corresponding BSE and Cs X-ray images of sample LP762h. These images were taken from a thin edge of the polished samples along which the synthetic glass of the slide substrate is partially

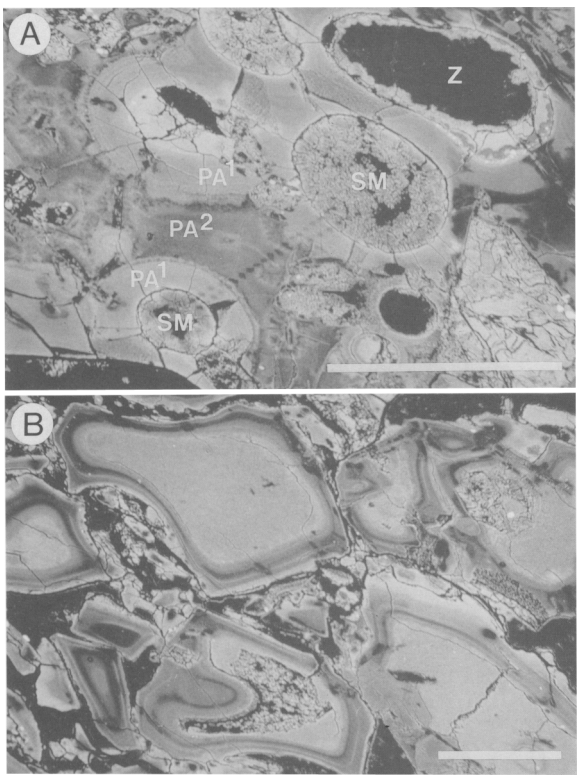

Figure 1. BSE micrographs of palagonitized glasses and smectite in hyaloclastite sample LP754K. A) amygdaloidal clast containing (Key:) SM = smectite; Z = zeolite; PA1 = high-Ti palagonitized glass; and PA2 = low-Ti palagonitized glass. B) zoned, palagonitized glassy clasts. Scale bar for A) is 500 μm and for B) is 200 μm.

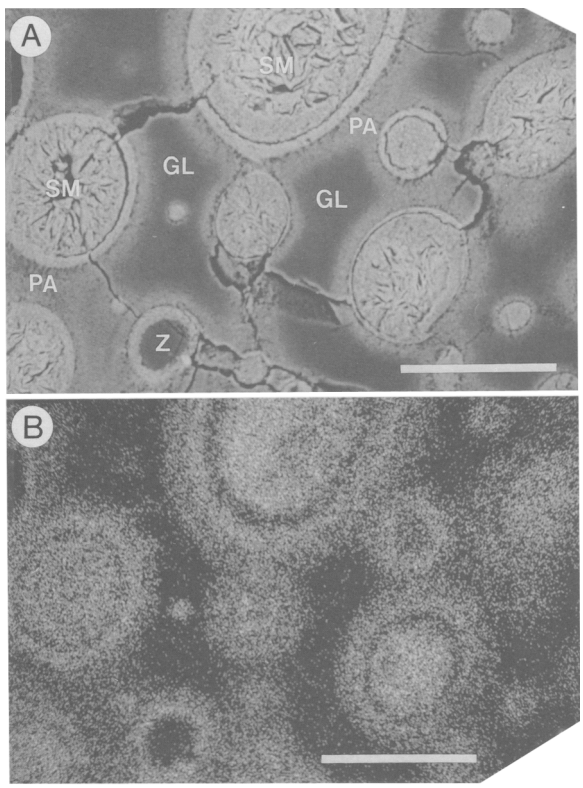

Figure 2. BSE micrograph A) and its complementary Cs-Lα X-ray dot map B) of hyaloclastite sample LP762H with (Key:) SM = amygdaloidal smectite: PA = palagonitized glass; and GL = microscope slide glass. Scale bars = 50 μm.

exposed between amygdules filled with smectite or zeolites, which are rimmed by palagonitized basaltic glass. In the BSE micrograph (Figure 2a), smectite exhibits the brightest tone; whereas the synthetic glass and zeolite exhibit the darkest tones and the palagonite is intermediate in gray level. The corresponding X-ray dot map shows that the smectite exhibits the greatest concentration of Cs and thus the highest CEC. The density of Cs X-rays in the palagonitized glass and therefore its CEC is notably lower. As expected, the synthetic glass and the zeolite did not accumulate Cs from the CsCl treatment. Figure 3 shows a similar pair of micrographs from sample LP754K. The BSE micrograph (Figure 3a) depicts an elongate amygdule filled with smectite, zeolite and apatite. The corresponding X-ray map shows that only the smectite and the palagonitized glass that encloses the amygdule have accumulated Cs from the CsCl treatment. In the holocrystalline samples, which do not contain palagonitized glass, smectite is the only mineral that exhibits CEC. Figure 4 shows a pair of micrographs from the interior of a basaltic pillow (sample LP 747a). Primary phases seen in the BSE image (Figure 4a) include plagioclase, clinopyroxene and Fe-Ti oxide; secondary phases include smectite and zeolite. Of all the crystalline phases, only smectite exhibits Cs-enrichment (Figure 4b).

Electron Microprobe Analyses

Representative quantitative analyses of smectite, corrensite and palagonitized glass are presented in Table 2. Compositional data are shown for the layer silicates and palagonite in both the pre- and post-CsCl treated states. Note that the pre- and post-CsCl pairs for each sample are not necessarily from the same locality in each polished mount.

Smectite from the La Palma sample suite is trioctahedral with Fe:Mg generally less than 0.5. In a study of the La Palma smectite, Schiffman and Staudigel (1995) noted that the sum of Al(VI) + Fe + Mn + Ti + Mg exceeded 6.0 for many of the microprobe spot analyses recalculated on a 22 O basis. For this reason, Schiffman and Staudigel (1995) hypothesized that significant Mg, up to 0.8 cations/22 O, may occupy an interlayer site, as opposed to octahedral sites in this smectite.

https://doi.org/10.1346/CCMN.1996.0440505 Published online by Cambridge University Press

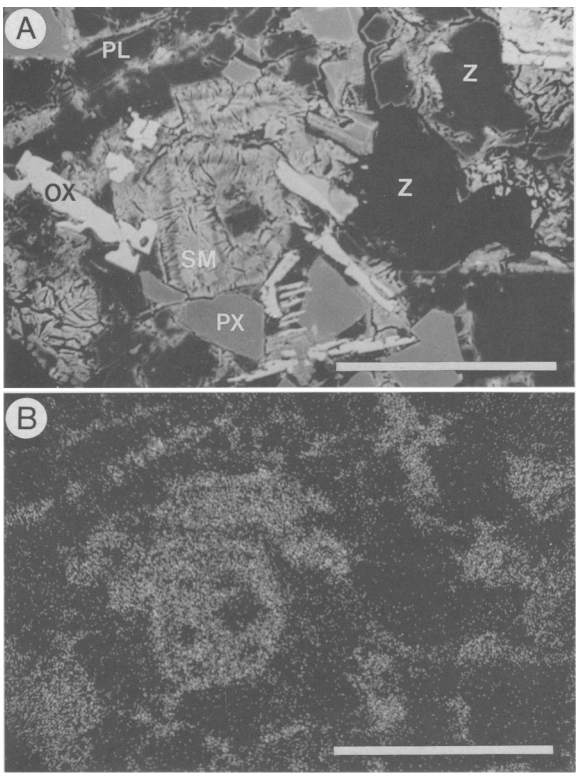

Figure 3. BSE micrograph A) and its complementary CsLα X-ray dot map B) of sample LP754K showing elongate vesicle in-filled by (Key:) SM = smectite; AP = apatite; and Z = zeolite; and PA = enclosed in palagonitized glass. Scale bars are 100 μm.

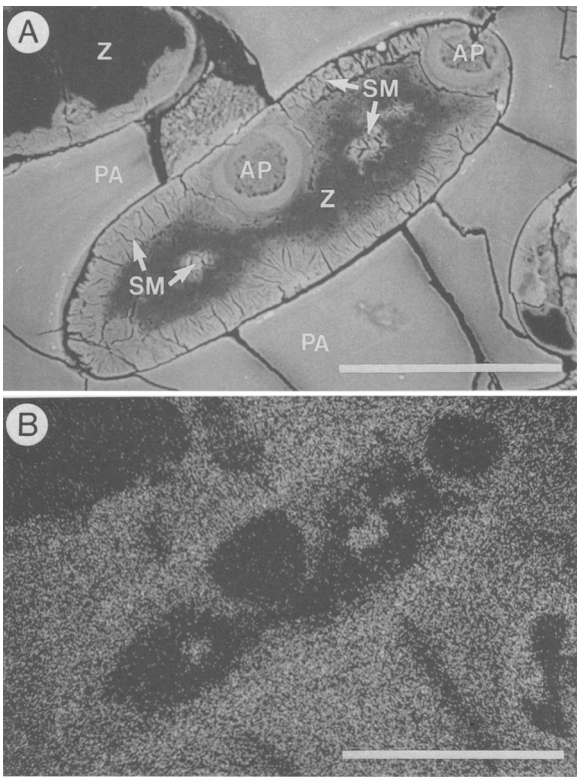

Figure 4. BSE micrograph A) and its complementary CsLα X-ray dot map B) of holocrystalline pillow basalt sample LP747a, exhibiting an intersertal texture characterized by (Key:) SM = smectite, which has replaced fine-grained mesostasis and primary mafic phenocrysts. Unaltered primary igneous minerals include (Key:) PL = calcic plagioclase; PX = clinopyroxene; and OX = Fe-Ti oxides; Z = zeolites fill vesicles. Scale bars are 100 μm.

Results of re-analysis of these samples after CsCl-saturation generally corroborate this hypothesis. After treatment, microprobe analyses indicate that the "excess" Mg, that is, beyond that which can be accommodated in 6 octahedral sites/22 O, decreased proportionally with the measured uptake of Cs, compared to before- and after-treatment analyses shown in Table 2. The CsCl-saturation also stripped the smectites of Na, K and most Ca. Although CsCl-saturation did not quantitatively remove all the "excess" Mg in the La Palma smectites, there is an obvious inverse correlation between the remaining "excess" Mg and the Cs fixed in the interlayer sites (Figure 5a). The Cs-concentrations in the La Palma smectite, which range from approximately 5 to nearly 16 wt% as Cs_2O (Table 2), correspond to CEC's between 60 and 120 meq/100 g (Table 1). The *in situ* measured CEC's of smectite from the three hyaloclastitic samples are all greater than the CEC of the smectite from the holocrystalline pillow basalt sample (LP747a, Table 1).

La Palma corrensite, a regular interstratification of tri-octahedral smectite and chlorite, is compositionally similar to smectite, especially in Fe:Mg (Schiffman and Staudigel 1995). However, the corrensite contains negligible "excess" Mg; Ca is the dominant interlayer cation (Table 2). Microprobe analyses of the corrensite after CsCl-treatment indicate that Ca is not quantitatively removed, although the remaining Ca exhibits a pronounced inverse correlation with Cs (Figure 5b). The mean CEC for the La Palma corrensite (35 meq/100 g in sample LP758b, Table 1) is lower than that of any measured for smectite, but the CEC of the smectite component of the corrensite is within the range of CEC for the other smectites within samples.

Although the CsCl-saturation experiments on smectite and corrensite yielded systematic correlations between Cs uptake and, respectively, Mg and Ca depletion, the results of *in situ* experiments on palagonitized glass are more equivocal. Since palagonite exhibits a broad composition range, which may vary greatly over distances of a few microns (Figure 6a–6d), it is difficult to relocate the exact sample volume for analysis after the CsCl treatment. However, aside from this difficulty, microprobe analyses clearly indicate that La

Palma palagonitized glass has a finite and, within a given sample, consistent CEC, ranging from approximately 30 to 60 meq/100 g (Tables 1 and 2).

Conventional CEC and Extractable Cation Analyses

Data from the 5 samples are presented in Table 1 and Table 3. Conventional CEC values for the < 2 μm size fractions are between 50 and 80 meq/100 g. Total extractable cation values for the < 2 μm fraction from these same samples, corrected where possible for extractable Ca due to $CaCO_3$ dissolution, range from approximately 50 to 95 meq/100 g. In 4 of the 5 samples, $CaCO_3$ constitutes less than approximately 1 wt% of the bulk sample. In the corrensite-bearing pillow basalt interior (sample LP758b), the percentage of $CaCO_3$ is too great (almost 13 wt%, Table 1) to allow an estimation of the extractable Ca from exchange sites versus solid-phase $CaCO_3$. In all of the samples, Ca is the dominant extractable cation (32 to 73 meq/100 g; Table 3), followed by Mg (3 to 13 meq/100 g), Na (0.5 to 10 meq/100 g) and K (0.4 to 1.5 meq/100 g).

DISCUSSION

CEC of Layer Silicates and Palagonitized Glass

The La Palma smectite generally has a high layer charge (Table 2, 0.8 to 2.0; Schiffman and Staudigel 1995), which approaches that of vermiculite. Nonetheless, these clays uniformly exhibit systematic smectite-like behavior in XRD analysis; they expand to 17 to 18 Å on glycerol solvation and collapse to 10 Å upon heating to 550 °C.

A comparison of CEC values determined by the *in situ* CsCl saturation technique, versus those determined by the conventional excess salt method is presented in Table 1. These 2 values can be compared directly for the holocrystalline pillow basalt samples, which do not contain palagonitized glass and in which layer silicates are the only materials that have extractable cation sites. Cation exchange by zeolites is probably not significant because zeolites do not occur to any significant extent in the clay fractions based upon XRD, and because cation exchange for Ca^{2+} and Cs^{+} is minimal for analcime (Baldar and Whittig 1968). For the smectite-bearing pillow basalt (747a), the mean *in situ* value (60 meq/100 g) agrees well with the conventionally-determined value (50 meq/100 g). For the corrensite-bearing pillow basalt (758b), the mean *in situ* value (35 meq/100 g) is nearly 30% less than the conventionally-determined value (52 meq/100 g). One possible explanation for this discrepancy can be seen in the data presented (Figure 5b). Electron microprobe analyses presented in Table 2, as well as by Schiffman and Staudigel (1995), indicate that for the La Palma corrensite, Ca is the dominant interlayer cation. But, the CsCl-treatments apparently did not result in complete Ca/Cs exchange. The most extensively exchanged corrensite still retains approximately 0.09 Cs/25 O (Figure 5b). Thus, the *in situ* data are conservative estimations of the corrensite CEC.

In the 3 samples that contain layer silicates as well as palagonitized glass, the direct comparison of *in situ* and conventional CEC results is not appropriate because the conventional CEC measures multiple exchanging components, whereas the *in situ* method is more discrete. However, the conventional CEC data, which reflect the mean CEC of the < 2 μm size fraction, should be bracketed by the *in situ* CEC values of smectite and palagonitized glass within that same sample (Table 1). Similarly, by mass balance, the 3 CEC values for each sample can be used to calculate an approximate mass ratio of smectite to palagonitized glass. Thus, in sample LP762h, the conventionally determined CEC value of 79 meq/100 g (Table 1) translates to a nearly 3 : 1 ratio of smectite/palagonite. Conversely, in sample LP743f, the conventionally determined value of 77 meq/100 g translates to a nearly 1: 3 ratio of smectite/palagonite. These ratios are corroborated by petrographic observations on the smectite/palagonitized glass within each of these samples (Table 1).

The range of CEC of palagonitized glass we determined by the *in situ* method (30 to 60 meq/100 g) is generally lower than that determined by conventional methods reported in previous studies (for example, Singer (1974) and Berkgaut et al. (1994) reported 60 to 100 meq/100 g). However, the conventional measurements reported in the literature were done on bulk "palagonite," which typically contains layer silicates of a presumably higher CEC than the palagonitized glass itself. Thus, conventional CEC measurements of "palagonite" clay fractions may over-estimate the CEC of the palagonitized glass itself.

Extractable Cations

A comparison of total extractable cations as determined 1) by leaching bulk samples with NH_4-acetate; and 2) estimated indirectly by electron microprobe analyses is presented in Table 3. This table presents three sets of values for extractable cation data on each element of interest: Ca, Mg, Na and K. Values listed in the first column of each elemental set (in units of meq/100 g) are those from NH_4-acetate extraction. In the second column, these data have been converted into units of charge per formula unit based on an average formula weight of 825 g for smectite and 950 g for corrensite. Re-calculated in this form, these values can be directly compared with the range in charge for each cation (third column of each set) determined from structural formulae obtained from electron microprobe analyses of the non-CsCl-saturated layer silicates. With one major exception, Mg, there is generally uniform agreement of the values determined by NH_4-acetate extraction and microprobe analyses. These results

https://doi.org/10.1346/CCMN.1996.0440505 Published online by Cambridge University Press

Table 2. Electron microprobe analyses, recalculated structural formulae and estimated cation exchange capacities of smectite, corrensite and palagonitized glass from La Palma metabasites.

	Smectite (22 O)						Corrensite (25 O)		Palagonitized glass (22 O)	
	LP743f pre-CsCl	LP743f post-CsCl	LP754k pre-CsCl	LP754k post-CsCl	LP762h pre-CsCl	LP762h post-CsCl	LP758b pre-CsCl	LP758b post-CsCl	LP743f post-CsCl	LP743f post-CsCl
SiO_2	38.45	37.05	41.02	37.45	41.54	36.34	35.99	34.23	34.31	34.44
Al_2O_3	12.68	11.95	11.19	9.54	12.35	9.81	13.98	12.99	13.39	10.41
FeO	19.18	12.89	14.12	12.06	15.00	15.89	19.33	19.19	18.50	14.48
MgO	16.15	13.92	20.00	17.04	15.55	13.05	18.44	18.05	13.00	8.62
MnO	0.36	0.14	0.08	0.09	0.11	0.09	0.34	0.09	0.08	0.12
TiO_2	0.03	0.00	0.04	0.01	0.11	0.06	0.02	0.00	1.11	8.29
CaO	1.14	0.15	1.28	0.45	0.97	0.09	1.04	0.68	0.83	8.05
Na_2O	0.10	0.01	0.17	0.00	0.15	0.03	0.00	0.04	0.00	0.07
K_2O	0.57	0.04	0.06	0.04	0.27	0.17	0.18	0.00	0.04	0.14
Cs_2O	0.00	15.65	0.00	9.36	0.00	12.72	0.00	4.74	8.36	6.42
Total	88.66	91.80	87.96	86.04	86.05	88.25	89.32	90.01	89.62	91.04
CEC		121		77		102		37	66	50
Si	5.98	6.25	6.22	6.35	6.42	6.35	6.34	6.28	5.74	5.61
Al IV	2.02	1.75	1.78	1.65	1.58	1.65	1.66	1.72	2.26	2.39
Al VI	0.30	0.63	0.22	0.25	0.68	0.37	1.24	1.09	0.38	0.00
Fe	2.50	1.82	1.79	1.71	1.94	2.32	2.85	2.94	2.59	1.97
Mg VI	3.15	3.50	3.97	4.03	3.36	3.29	4.84	4.94	2.88	2.10
Mn	0.05	0.02	0.01	0.01	0.01	0.01	0.05	0.01	0.01	0.02
Ti	0.00	0.00	0.01	0.00	0.01	0.01	0.00	0.00	0.14	1.02
Sum VI	6.00	5.97	6.00	6.00	6.00	6.00	8.98	8.98	6.00	5.11
Mg IL	0.59	0.00	0.54	0.27	0.23	0.11	0.00	0.00	0.36	0.00
Ca	0.19	0.03	0.21	0.08	0.16	0.02	0.20	0.13	0.15	1.41
Na	0.03	0.00	0.05	0.00	0.05	0.01	0.00	0.01	0.00	0.02
K	0.11	0.01	0.01	0.01	0.05	0.04	0.04	0.00	0.01	0.03
Cs	0.00	1.13	0.00	0.68	0.00	0.95	0.00	0.37	0.60	0.45
Sum IL	0.92	1.17	0.81	1.04	0.49	1.13	0.24	0.51	1.12	1.91
IL charge	1.70	1.20	1.56	1.39	0.88	1.26	0.44	0.64	1.63	3.32

imply that the layer silicates are the main source of extractable cations in the these samples, and/or that during treatment of bulk samples with NH_4-acetate, the palagonitized glass is contributing extractable cations congruently with that implied by the proportions of interlayer cations, especially Ca, Na and K, from the layer silicates.

However, there is an order of magnitude less Mg extracted by NH_4-acetate than expected from the electron microprobe analyses of smectite (Table 3). This is the case in all the smectite-bearing samples, even LP743f, for which the *in situ* CEC data indicate that Cs has completely exchanged with Mg and thus implying that Mg should be readily extractable by NH_4-acetate treatment. In other samples, which show less complete Cs/Mg exchange in smectite (Figure 5a), it is possible that some of the "excess" Mg may not occupy exchangeable/extractable hydrated, interlayer sites in the smectite. Rather, these Mg cations could occur in brucite-like layers, which would indicate the development of minor chlorite interstratification with smectite (Bailey 1982). Small amounts, that is, <10%, of chlorite interlayering are not precluded by the results of XRD analysis (apparently clean smectite) for the La Palma samples (Schiffman and Friedleifsson 1991), although the amount of interlayered brucite required to explain the discrepancy between the Mg data sets in Table 3 would certainly be reflected in systematic differences in the XRD behavior of these clays. Non-crystalline remnants within the smectite would probably cause at least some XRD peak broadening, but we did not evaluate this effect.

Since the cations extracted by NH_4-acetate treatment are a combination of those contributed by layer silicates as well as the palagonitized glass, it is possible that the high Mg/Ca extractable cation ratios implied by the smectite structural formulae (Tables 2 and 3) could be offset by an antithetically low Mg/Ca for the palagonitized glass. In Table 2, the palagonitized glass analyses have been arbitrarily recalculated on a 22 O basis—the same used for smectite structural formulae. Previous workers (Jercinovic et al. 1990; Zhou et al. 1992) have argued that palagonitized glass has a proto-smectite-like structure containing crystallites of both di- and tri-octahedral 2:1 layer silicates. The recalculated analyses in Table 2 are consistent with these findings: the sum of octahedral Al + Fe + Ti + Mn + Mg in the La Palma palagonitized glass is generally between 4.7 and 6.4 cations/22 O. If these recalculated palagonitized glass analyses have any further structural analogy with smectite, it might be predicted that more Ca than Mg would be extracted in the La Palma

https://doi.org/10.1346/CCMN.1996.0440505 Published online by Cambridge University Press

Table 2. Extended.

Palagonitized glass (22 O)					
LP754k pre-CsCl	LP754k post-CsCl	LP754k pre-CsCl	LP754k post-CsCl	LP762h post-CsCl	LP762h post-CsCl
35.76	35.05	47.10	46.72	36.79	34.25
9.33	9.18	16.68	15.68	10.81	9.80
11.55	12.14	10.44	9.87	15.54	13.47
8.99	8.99	9.66	9.13	10.57	9.37
0.23	0.10	0.14	0.00	0.10	0.19
9.38	8.42	1.33	1.63	2.98	8.25
12.05	10.78	3.77	3.92	4.79	9.45
0.16	0.07	3.50	2.88	0.16	0.01
0.10	0.05	0.18	0.21	0.32	0.32
0.00	3.98	0.00	3.94	7.58	4.15
87.55	88.76	92.80	93.98	89.64	89.26
	32		30	60	33
5.68	5.71	6.62	6.70	6.08	5.59
1.75	1.76	1.38	1.30	1.92	1.89
0.00	0.00	1.38	1.35	0.19	0.00
1.53	1.65	1.23	1.18	2.15	1.84
2.13	2.18	2.03	1.95	2.60	2.28
0.03	0.01	0.02	0.00	0.01	0.03
1.12	1.03	0.14	0.18	0.37	1.01
4.81	4.87	4.80	4.66	5.32	5.16
0.00	0.00	0.00	0.00	0.00	0.00
2.05	1.88	0.57	0.60	0.85	1.65
0.05	0.02	0.95	0.80	0.05	0.00
0.02	0.01	0.03	0.04	0.07	0.07
0.00	0.28	0.00	0.24	0.53	0.29
2.12	2.19	1.55	1.68	1.50	2.01
4.17	4.07	2.12	2.28	2.35	3.66

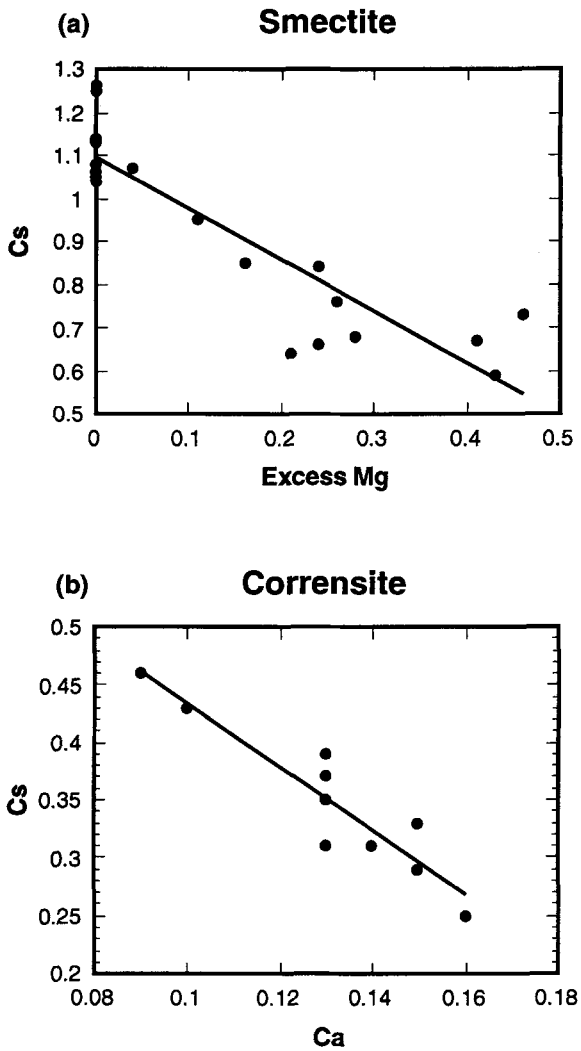

Figure 5. Results of *in situ* CEC experiments by CsCl-treatment. A) Cs versus "excess" Mg [that remaining after the 6 octahedral sites/22 O have been filled with Al(VI), Ti, Mn and Fe] in smectite; B) Cs versus Ca in corrensite (25 O basis).

palagonitized glass, since most of the recalculated palagonitized glass analyses in Table 2 contain over 1 Ca/22 O and none contain "excess" Mg (for a trioctahedral-like structure). However, the NH_4-acetate extraction data, even for the most palagonite-rich sample, that is, LP 743f, which contains roughly a 3:1 ratio of palagonite:smectite, do not support this: the amount of extractable Ca is roughly that predicted from smectite structural formulae alone. The observed lack of correlation between the NH_4-acetate extraction and *in situ* Ca:Mg ratios may be a result of the former technique, although $BaCl_2$ extractions on these same bulk samples did not produce significantly different results (Southard 1995, unpublished data). Specifically, the extraction techniques may preferentially leach Ca with respect to Mg if the latter cations are not fully in exchangeable sites. We propose that Mg may occupy remnant network-modifying sites within the tectosilicate-like structure of the original (now palagonitized) basaltic glass, and thus be preferentially resistant to both NH_4-acetate and Cs extraction techniques. Alternatively, the high Mg charge as indicated by the microprobe analyses of smectite (Table 3) in all the La Palma samples may not be representative of the entire population of smectite in these samples. That is, smectite which does not occur in coarse aggregates (for example, that coating grain boundaries and thus volumetrically significant) and which was not analyzed, might have an insignificant amount of interlayer Mg with respect to Ca.

The results of the *in situ* CEC analyses on the palagonitized glass in sample LP754K do offer some clues regarding which elements are actually being extracted when Cs is exchanged into this material. Figure 6 shows concentration profiles of 4 elements determined from microprobe analyses before and after CsCl-saturation. The concentration profiles begin (to the left) and terminate (to the right) within the 2 rounded smectite aggregates labeled "SM" in Figure 1a. The palagonitized glass is markedly zoned in composition. The smectite aggregates are encircled by ap-

https://doi.org/10.1346/CCMN.1996.0440505 Published online by Cambridge University Press

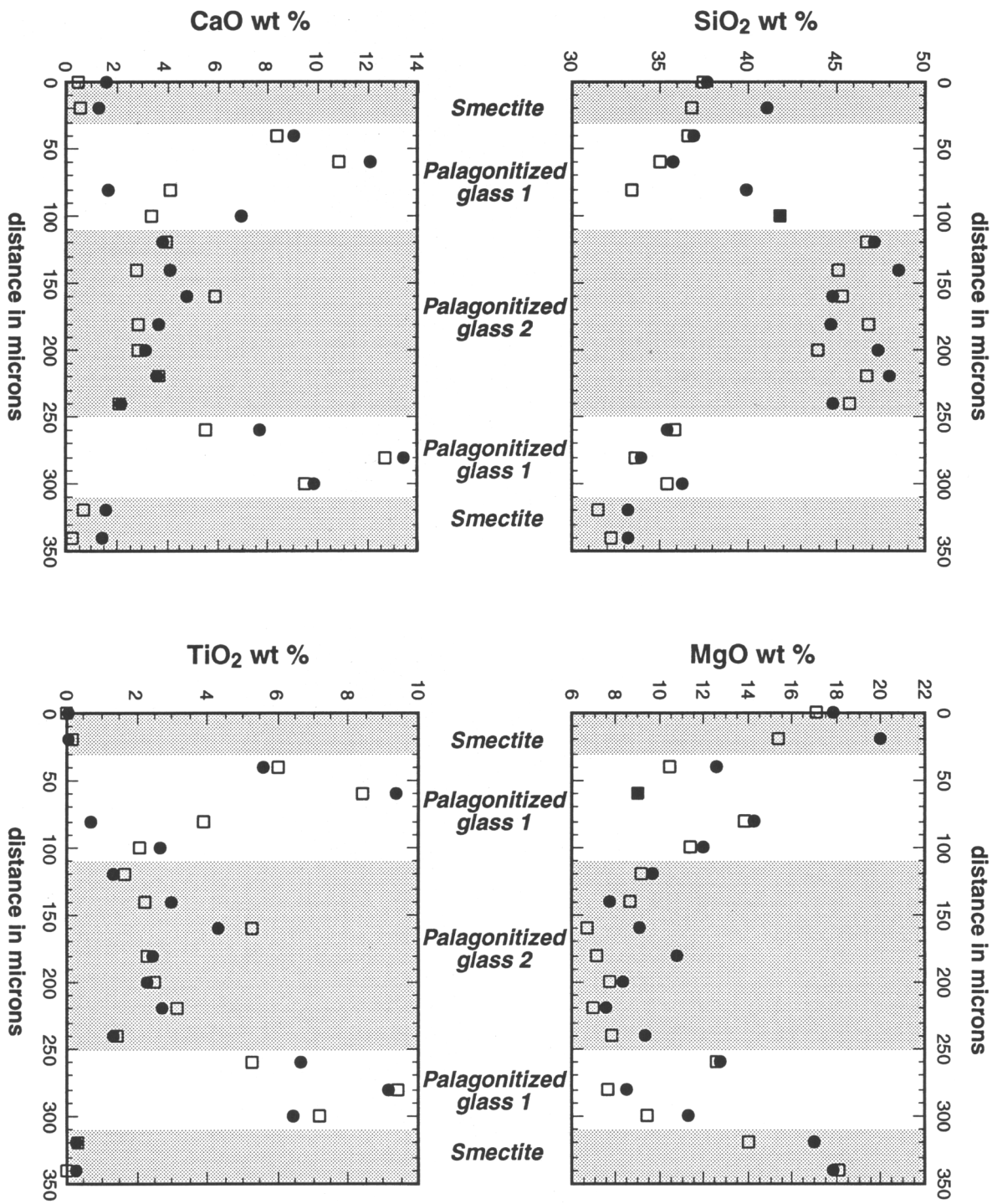

Figure 6. Results of electron microprobe elemental traverses depicting compositional variations for A) SiO_2; B) MgO; C) CaO; and D) TiO_2 in hyaloclastite sample LP754k. The traverse, from lower left to upper right, begins and ends within the 2, labeled smectite aggregates seen in Figure 1A, and crosses 2 types of palagonitized glass: high-Ti (PA1) and low-Ti (PA2). Key: Filled circles = pre-CsCl-saturation results; open squares = results after CsCl-saturation; and filled squares = negligible compositional change occurred after CsCl-saturation.

https://doi.org/10.1346/CCMN.1996.0440505 Published online by Cambridge University Press

Table 3. Comparison of *in situ* charge characteristics determined by microprobe with bulk extractable cations.

	Ca bulk meq†	Ca bulk charge§	Ca probe charge¶	Mg bulk meq	Mg bulk charge	Mg probe charge#	Na bulk meq	Na bulk charge	Na probe charge	K bulk meq	K bulk charge	K probe charge
LP743f	31.7	0.3	0.1–0.3	13.3	0.11	1.1–1.6	2.2	0.02	0.01–0.05	0.7	0.01	0.11–0.18
LP747a	42.0	0.3	0.2–0.6	6.2	0.05	0.0–1.8	7.0	0.06	0.04–0.63	1.0	0.01	0.04–0.25
LP754k	73.3	0.6	0.2–0.7	10.3	0.08	0.2–1.6	10.2	0.08	0.03–0.05	1.5	0.01	0.01–0.05
LP758b	ND‡	ND	0.4–0.5	3.0	0.03	0.0–0.1	0.5	0.00	0.00–0.03	0.4	0.00	0.00–0.04
LP762h	45.4	0.4	0.2–0.5	11.4	0.09	0.4–1.6	4.7	0.04	0.02–0.05	0.8	0.01	0.01–0.15

† Cations extracted with 1 *M* NH_4 acetate at pH 7.0 on <2 mm fraction; Ca adjusted for dissolution of $CaCO_3$; units are meq/100 g.

‡ The extractable Ca in sample LP758b is not determinable (ND) because Ca potentially produced by $CaCO_3$ dissolution (256 meq/100 g) exceeded that extracted by NH_4 acetate (31 meq/100 g).

§ Calculated from bulk extractable cation data by assuming 825 g/formula unit for smectite and 950 g/formula unit for corrensite.

¶ Range of layer charge as implied by structural formulae from electron microprobe analyses of layer silicates.

Mg in this column is that remaining after octahedral sites are completely filled with non-tetrahedral Al, Fe, Ti, Mn and Mg.

proximately 100 mm thick bands of isotropic, Ca- and Ti-rich palagonitized glass ("PA 1" in Figure 1a and "palagonitized glass 1" in Figure 6), which themselves are enclosed within slightly birefringent palagonitized glass ("PA 2" in Figure 1a and "palagonitized glass 2" in Figure 6), whose composition more closely approximates basaltic (compare third and fifth palagonitized glass analyses in Table 2).

Both varieties of palagonitized glass described above have approximately the same CEC (that is, 30 to 35 meq/100 g as measured by the *in situ* method (Table 1); although it is unclear which cations are displaced by Cs. From the compositional data on both types of palagonitized glass shown in Figure 6, only Mg exhibits a consistent pattern of depletion in the post-versus pre-CsCl treated state. Specifically, MgO is depleted (relative to its abundance in the pre-treated palagonitized glass) in 11 of the 14 analyses within the traverse shown in Figure 6. Although these depletions are as large as 2 to 3 wt% MgO, that is, within the central portion of the palagonitized glass 2 zone (Figure 6), most of the observed depletions are less than 1 wt%. The CaO is depleted in 6 of the 7 analyses from the type 1 palagonitized glass, in amounts up to 4 wt%, but from only 2 of the 7 analyses in the type 2 palagonitized glass. No other element (including K_20, Na_2O, Al_2O_3 and FeO, which are not shown on Figure 6) is depleted, relative to its pre-treated abundance, in more than 8 of the 14 analyses.

Can the measured MgO and CaO depletions account for the 30 to 35 meq/100 g CEC as indicated by the *in situ* CEC results? A loss of 0.5 wt% MgO in palagonitized glass, typical of the results from the *in situ* exchange experiments, is equivalent to approximately 0.1 Mg/22 O; a loss of 1.25 wt% CaO is equivalent to approximately 0.2 Ca/22 O (Table 2). The measured *in situ* CEC's of 30 to 35 meq/100 g, which are apparently constant for both types of the palagonitized glasses, correspond to contents of between 0.2 to 0.4 equivalents of Cs/22 O (Table 2). Therefore, exchangeable Mg and/or Ca generally cannot account for the entire measured *in situ* CEC of the palagonitized glass. One possibility that should be further investigated, is that the negative structural charge of the palagonitized glass is partially neutralized by H protons, which may readily exchange with network modifying cations during the onset of silicate glass dissolution (Petit et al. 1990), and which are not detectable by electron microprobe analysis.

CONCLUSIONS

1) Electron microprobe analyses suggest that the La Palma smectite has appreciable interlayer Mg and are corroborated by the results of *in situ* CEC measurements.

2) The *in situ* experiments on 3 hyaloclastite samples indicate that palagonitized glass has a lower CEC (30 to 35 meq/100 g) than smectite (65 to 120 meq/100 g). The CEC's of the <2 μm size fractions in these hyaloclastites, as obtained by the conventional excess salt method, are bracketed by the *in situ* measured CEC's of layer silicates and palagonitized glass.

3) Exchangeable cations, for example, Mg in smectite and Ca in corrensite, are not completely replaced by Cs during the *in situ* experiments, indicating that the *in situ* method may yield conservative estimates of the CEC's for the layer silicates. Further, some of the Mg allocated to interlayer positions may actually occupy brucite-like octahedral positions that are not exchangeable by Cs. The apparent lack of stoichiometric exchange of Cs for interlayer cations may also be due to the presence of exchangeable protons that are not measured by the microanalytic techniques.

4) The sums of cations extracted by NH_4-acetate on bulk samples are generally similar to the CEC determined by both the excess salt and *in situ* methods. Except for Mg, the proportions of NH_4-extractable cations are similar to those predicted from the stoichi-

https://doi.org/10.1346/CCMN.1996.0440505 Published online by Cambridge University Press

ometry of layer silicates. The *in situ* experiments on palagonitized glass indicate that some Mg and Ca may exchange for Cs, although the NH_4-acetate extractions do not corroborate this. This discrepancy may be attributable to Mg and Ca, which occupy remnant network-modifying sites within the tectosilicate-like structure of the original (now palagonitized) basaltic glass, and thus are resistant to extraction with NH_4-acetate. Alternatively, the (high) extractable Mg-content of the smectite as implied by electron microprobe analyses may not be representative of all the smectite in these samples.

ACKNOWLEDGMENTS

Schiffman's work on layer silicate mineralogy has been supported by NSF grant EAR-9203743, Southard's by Hatch project CA-D*-LAW-4525-H. Thanks to H. Staudigel and J. Gee for their help with field work in La Palma and subsequent petrographic study of these metabasites, and to S. Munn for her help with lab work. Thanks to S. Hillier for telling P. Schiffman about the *in situ* CEC method. Reviews by S. Hillier and W. Lynn improved the clarity and content of this manuscript.

REFERENCES

Bailey SW. 1982. Nomenclature for regular interstratifications. Am Mineral 67:394–398.

Baldar NA, Whittig LD. 1968. Occurrence and synthesis of soil zeolites. Soil Sci Soc Am J 32:235–238.

Berkgaut V, Singer A, Stahr K. 1994. Palagonite reconsidered: paracrystalline illite-smectites from regoliths on basic pyroclastics. Clays Clay Miner 42:582–592.

Bilgrami SA, Howie RA. 1960. The mineralogy and petrology of a rodingite dyke, Hindubaugh, Pakistan. Am Mineral 45:791–801.

Dimroth E, Lichtblau AP. 1979. Metamorphic evolution of Archean hyaloclastites, Noranda area, Quebec, Canada. Part I: Comparison of Archean and Cenezoic sea-floor metamorphism. Can J Earth Sci 16:1315–1340.

Furnes H. 1984. Chemical changes during progressive subaerial palagonitization of a subglacial olivine tholeiite hyaloclastite: A microprobe study. Chem Geol 43:271–285.

Golden DC, Morris RV, Ming DW, Lauer HV, Jr., Yang SR. 1993. Mineralogy of three slightly palagonitized basaltic tephra samples from the summit of Mauna Kea, Hawaii. J Geophys Res 98:3401–3411.

Hay RL, Iijima A. 1968. Petrology of palagonitic tuffs of the Koko Craters, Oahu, Hawaii. Contributions Mineral Petrol 17:141–154.

Hillier S, Clayton T. 1992. Cation exchange 'staining' of clay minerals in thin-section for electron microscopy. Clay Miner 27:379–384.

Jackson ML. 1979. Soil chemical analysis-Advanced course, 2nd. ed. Madison, WI: M.L. Jackson. 895 p.

Jakobsson SP, Moore JG. 1986. Hydrothermal minerals and alteration rates at Surtsey volcano, Iceland. Geol Soc Am Bull 97:648–659.

Jercinovic MJ, Keil K, Smith MR, Schmitt RA. 1990. Alteration of basaltic glasses from north-central British Columbia, Canada. Geochim Cosmochim Acta 54:2679–2696.

Kinter EB, Diamond S. 1966. A new method for preparation and treatment of oriented-aggregate specimens of soil clays for x-ray diffraction analysis. Soil Sci 81:111–120.

Petit J-C, Della Mea G, Dran J-C, Magonthier M-C, Mando PA. Paccagnella A. 1990. Hydrated-layer formation during dissolution of complex silicate glasses and minerals. Geochim Cosmochim Acta 54:1941–1955.

Schiffman P, Fridleifsson GO. 1991. The smectite to chlorite transition in drillhole NJ-15, Nesjavellir geothermal field, Iceland: XRD, BSE, and electron microporbe investigations. J Metamor Geol 9:679–696.

Schiffman P, Staudigel H. 1995. The smectite to chlorite transition in a fossil seamount hydrothermal system: the Basement Complex of La Palma, Canary Islands. J Metamor Geol 13:487–498.

Schiffman P, Staudigel H. 1994. Hydrothermal alteration of a seamount complex on La Palma, Canary Islands: Implications for metamorphism in accreted terranes. Geology 22: 151–154.

Singer A. 1974. Mineralogy of palagonitic material from the Golan Heights, Israel. Clays Clay Miner 22:231–240.

Soil Survey Staff. 1992. Soil Survey Laboratory Methods Manual: Soil Survey Investigations Report 42, V. 2.0. USDA-Soil Conservation Service, Lincoln, NE. 400 p.

Southard RJ. 1995. Department of Land, Air and Water Resources, University of California-Davis, Davis, CA 95616.

Staudigel H. 1981. Der basale Komplex von La Palma. Submarine vulkanische prozesse, Petrologie, Geochemie und sekundare prozesse im herausgehobenen, submarinen Teil einer ozeanischen Insel [Ph.D. thesis]. Bochum, Germany: Ruhr University. 357 p.

Staudigel H, Hart SR. 1983. Alteration of basaltic glass: mechanisms and significance for the oceanic crust-seawater budget. Geochim Cosmochim Acta 47:337–350.

Staudigel H, Schmincke H-U. 1984. The Pliocene Seamount series of La Palma/Canary Islands. J Geophys Res 89: 11915–11215.

Thorseth IH, Furnes H, Tumyr O. 1995. Textural and chemical effects of bacterial activity on basaltic glass: an experimental approach. Chem Geol 119:139–160.

Thorseth IH, Furnes H, Tumyr O. 1991. A textural and chemical study of Icelandic palagonite of varied composition and its bearing on the mechanism of glass-palagonite transformation. Geochim Cosmochim Acta 55:731–749.

Whittig LD, Allardice WR. 1986. X-ray diffraction techniques. Methods of soil analysis, Part 1: Physical and mineralogic methods, Agronomy Monograph no. 9. American Society of Agronomy—Soil Science of America. p 331–362.

Zhou Z, Fyfe WS. 1989. Palagonitization of basaltic glass from DSDP Site 335, Leg 37: Textures, chemical composition, and mechanism of formation. Am Mineral 74:1045–1053.

Zhou Z, Fyfe WS, Tazaki K, van der Gaast SJ. 1992. The structural characteristics of palagonite from DSDP Site 335. Can Mineral 30:75–81.

(Received 13 October 1995; accepted 20 December 1995; Ms. 2699)